

Phase Separation Induced by Conformational Ordering of Gelatin in Gelatin/Maltodextrin Mixtures

N. Lorén,[†] A.-M. Hermansson,^{*,†} M. A. K. Williams,[‡] L. Lundin,[‡] T. J. Foster,[‡] C. D. Hubbard,[‡] A. H. Clark,[‡] I. T. Norton,[‡] E. T. Bergström,[§] and D. M. Goodall[§]

SIK, The Swedish Institute for Food and Biotechnology, Box 5401, SE-402 29 Gothenburg, Sweden; Unilever Research Colworth, Colworth House, Sharnbrook, Bedford, MK44 4LQ, UK; and Department of Chemistry, University of York, Heslington, York, YO10 5DD, UK

Received July 25, 2000

ABSTRACT: Mixtures of gelatin and maltodextrin in aqueous solution have been quenched to temperatures at which they are initially miscible but where gelatin ordering is initiated. In many cases phase separation was observed to occur after a significant time delay, and the dependence of these delays on quench temperature and biopolymer concentration has been studied in detail using turbidity measurements and confocal laser scanning microscopy (CLSM). Furthermore, by observing the optical rotation (OR) and turbidity of the system simultaneously, the gelatin helix content and the time delay before the onset of phase separation were monitored concurrently. The observed delay times were found to correspond to the time taken for the development of a certain degree of gelatin ordering, which drives the separation process. A further consequence of gelatin ordering is the viscosifying of the solution and, at sufficient concentrations, the formation of a gel. Therefore, rheological measurements have been used in addition to turbidity measurements and CLSM in order to monitor further the structural development of the systems. A comparison of the data obtained from these techniques shows that while the development of a certain elasticity will trap the system morphology, this elasticity is not directly related to that found at the gel point. At low maltodextrin concentrations, where phase separation was not detected by turbidity, transmission electron microscopy (TEM) has been used to examine the microstructure on a smaller length scale.

Introduction

Many mixed biopolymer systems are incompatible and phase separate in aqueous solution. In addition, such systems are often studied under conditions where at least one of the components will form a gel. In these cases previous work has shown that the morphology of mixed biopolymer systems depends on the relative rates of phase separation and gel formation.^{1–3} For systems that are incompatible at temperatures above the gelation temperature of the components, phase separation can proceed rapidly, equilibrating concentrations and phase volumes. Subsequently, the morphology coarsens by coalescence and/or Ostwald ripening and ultimately results in sedimentation and creaming. For systems of this type it is likely that the major effect of quenching directly to temperatures below the gelation temperature of the gelling component is that coarsening will be slowed and ultimately arrested by the formation of a network. Alternatively, if phase separation only occurs after the initiation of the ordering or network formation of the gel-forming component, then, while the viability of coarsening mechanisms will be strongly influenced, the phase separation itself may also be inhibited and the system trapped in a nonequilibrium state by gelation. Consequently, knowledge of the time of onset of phase separation at a particular temperature, in relation to the progress of the gel formation, is crucial for understanding the generated morphology and the material properties of phase-separated biopolymer mixtures.

Previously some effort has been made in outlining approaches for the coupling of phase separation and gelation.^{4–12} However, while the majority of the papers in this area have focused on network formation as an arresting mechanism for phase separation, the main aim of this article is to examine the possible promoting effect of the conformational ordering of gelatin on the onset of demixing. At present there has been relatively little work in this direction. Mixed solutions of gelatin and dextran^{1,13} have been studied following quenches performed to temperatures both above and below the gelatin gelation temperature and the phase separation kinetics, as determined by small-angle light scattering, were found to be different in these cases. All the systems studied were intrinsically immiscible at temperatures well above the ordering temperature of gelatin, so that in this case it is difficult to draw any conclusions about the effect of ordering on the onset of demixing. It has however been suggested that mixtures of κ - and ι -carrageenan phase separate as a direct consequence of the ordering process of either of the polysaccharides.¹⁴ Other previous studies of the phase behavior of the gelatin/maltodextrin systems have focused on the effect of different thermal treatments and gelatin types on the morphology of the final system,¹⁵ on the incompatibility at temperatures well above the gelatin ordering temperature,¹⁶ and on the occurrence of phase inversion.³

In the field of synthetic polymers it has been shown that the phase separation of mixed systems can be induced by various procedures. The conventional procedure is to perform a thermal quench into the incompatibility region of the phase diagram.¹⁷ Other related procedures include compositional quenches,^{18,19} pressure jumps,²⁰ and nonsolvent-induced phase separation.^{21,22} Phase separation has also been induced by methods

[†] The Swedish Institute for Food and Biotechnology.

[‡] Unilever Research Colworth.

[§] University of York.

* To whom correspondence should be sent.

more akin to conformational ordering and network formation, such as intramolecular photoisomerization of the individual polymers^{23–27} and intermolecular photodimerization. In polymerization-induced phase separation (PIPS),^{28–33} the incompatibility is induced following the initiation of a chemical reaction that polymerizes one of the components of a binary mixture. The main driving force toward incompatibility in PIPS is the loss in entropy due to the progressive increase in molecular weight of the component that polymerizes.³⁴

The gelatin/maltodextrin system used in this study is an archetypal system for the study of ordering-induced phase separation as it is possible to initiate demixing both below and above the gelation temperature of gelatin just by a small change in composition.² In addition, it is easy to influence the progress of ordering and gel formation by simply adjusting the temperature. Recent studies of the temperature dependence of the gelatin/maltodextrin phase diagram with and without salt addition^{2,35–37} have shown indications of additional driving forces toward phase separation owing to the conformational ordering of gelatin. In this paper we aim to demonstrate unequivocally that such ordering is capable of inducing demixing, by simultaneously monitoring the biopolymer ordering and system miscibility.

Experimental Section

Sample Preparation. The gelatin sample was a lime-treated gelatin (LH) supplied by SKW (Baupre, France). Using size-exclusion chromatography coupled with light scattering, $M_n = 83\,300$ and $M_w = 146\,000$ g mol⁻¹ were found. The maltodextrin was a DE 2 grade (SA2) supplied by Avebe (Foxhol, Holland). From the DE value, M_n was estimated to be about 9000 g mol⁻¹. The moisture content (10% for maltodextrin and 12.4% for gelatin) was taken into account for the preparation of all solutions.

Biopolymer solutions were prepared as follows: SA2 powder was first dispersed in cold water and dissolved while stirring at 95 °C for 30 min. Gelatin was prepared similarly, but not heated above 60 °C (70 °C for the CLSM experiments), to prevent any thermal degradation. SA2 solutions were cooled to 60 °C for 5 min and then mixed with the gelatin solution in order to obtain the desired % w/w of materials in the mixed solution. Mixtures were stirred for 5–10 min more before the introduction of the sample into the appropriate instrument of study.

Simultaneous Optical Rotation/Turbidity Measurements. Optical rotation measurements were performed using a polarimeter based on the Faraday modulation technique. The instrument monitors both rotation in the plane of polarization and transmittance of the laser beam through the sample, thus allowing simultaneous monitoring of both optical rotation and turbidity changes. The optical layout is similar to that for Faraday modulation polarimetry described in previous work.^{38,39} A 35 mW 820 nm diode laser module (model DC25F, Spindler & Hoyer) was used as the light source for these studies.

A cylindrical stainless steel cell with a diameter of 0.5 cm and a 2.5 cm path length was used which was thermostated with water circulating through the cell body. Quenches were performed using two water baths (Julabo F25 and Grant KD/TD-P) by switching flow to the cell from one to the other. The temperature of the cell contents was found to follow an exponential course to the target temperature with 90% of the temperature change occurring in 1.1 min. Temperature jump experiments with maltodextrin solutions were carried out so that any OR changes caused by the temperature dependence of the maltodextrin optical activity and temperature-induced artifact signals from differential stress on the cell windows could be measured. In addition, temperature jump experiments with a gelatin solution from 60 to 50 and 40 °C, both above

the ordering temperature, enabled the temperature dependence of the OR of gelatin in the disordered state to be measured. The value was found to be 1.5 m° K⁻¹ for a 4% solution in the 2.5 cm cell at 820 nm. Any additional OR change observed in gelatin–maltodextrin mixtures when jumped from 60 °C to below the gelatin ordering temperature was attributed to helix formation of gelatin. The amount of helix formation was calculated assuming a value for OR change, at 820 nm, of 1.2° for 100% helix. This value is based on the cell path length, the gelatin concentration used, and the literature value of the OR of collagen solutions at 436 nm, with corrections made for the change in wavelength.⁴⁰

Turbidity Measurements. All measurements reported here were carried out using a Perkin-Elmer Lambda 40 spectrophotometer. The apparent acceptance angle of the experimental setup was measured using standard latex spheres as described previously³⁶ and was found to be approximately 3°. To estimate particle sizes, the turbidity was measured as a function of wavelength between 600 and 800 nm, and the spectra thus obtained were fitted using a method described in detail elsewhere.³⁶

A custom temperature controlled cell holder was used. This consisted of a copper cell holder, the temperature of which could be controlled by Peltier devices driven by a remote controllable dual polarity power supply. The output current was controlled via a standard controller (WEST 4400) running a conventional P.I.D algorithm. Feedback was taken from a platinum resistance thermometer (PT100) embedded in the copper cell holder. Another PT100 was incorporated into the arrangement that fitted into the cuvette and measured the temperature of the fluid at a known cell height. Both temperature sensors were calibrated to ± 0.2 °C and the values read via a serial interface to a PC. The typical cooling rate for a 5 mm path length cuvette was 16 °C min⁻¹. Further details of the temperature control system are given elsewhere.³⁷

Confocal Laser Scanning Microscopy. The CLSM system used consists of a Leica TCS 4D confocal laser scanning microscope (Heidelberg, Germany), equipped with a Linkam TMS 92 heating and cooling table. The emission maximum of the argon–krypton laser used as the light source was 488 nm. On the basis of the size of the dispersed phase, the microscope objective having a magnification of 63 times and a computer zooming of 3.97 \times were used. The signal from the sample was collected with the TRITC filter (LP-590) and the fast scanning mode. Eight scans were averaged during the creation of an image. After acquisition, the images were transferred to a SUN Ultra1 workstation and stored on hard disk. Finally, a Contextvision microGOP 2000/S (Linköping, Sweden) contextual image analysis system was used to analyze the images taken.

Maltodextrin was covalently labeled with rhodamine B isothiocyanate (RITC) to improve the fluorescence intensity^{2,41,42} and used in sample preparation as described above. Thereafter, the mixed solutions were transferred immediately to a 60 °C preheated cup in the CLSM microscope. This cup was immediately covered by an 80 °C preheated cover glass to prevent cooling-induced phase separation close to the surface. The cups used were made of metallic material with high thermal conductivity and had an inner diameter of 14.2 mm, a depth of 1.8 mm, and thus a sample volume of 0.29 mL. Finally, the sample was equilibrated for a few min at 60 °C and then cooled from 60 °C to the quench temperature at 30 °C min⁻¹. Following the start of the quench, images were acquired every 1.43 s until the main structural evolution had finished.

Transmission Electron Microscopy. RITC-labeled maltodextrin and gelatin were mixed as for the CLSM. The gelatin/RITC-maltodextrin solution was cooled in a LINKAM cooling stage, and the behavior was studied in the CLSM before preparation for TEM. The gel was fixed in 2% glutaraldehyde. The gel was then postfixated in 2% osmium tetroxide. The water in the gel was exchanged for ethanol in a series of solutions of increasing concentrations of ethanol. The samples were embedded in TAAB 812 resin (Berkshire, England), and the polymerization was carried out at 60 °C for 24 h. The plastic-embedded gels were then thin-sectioned for TEM using

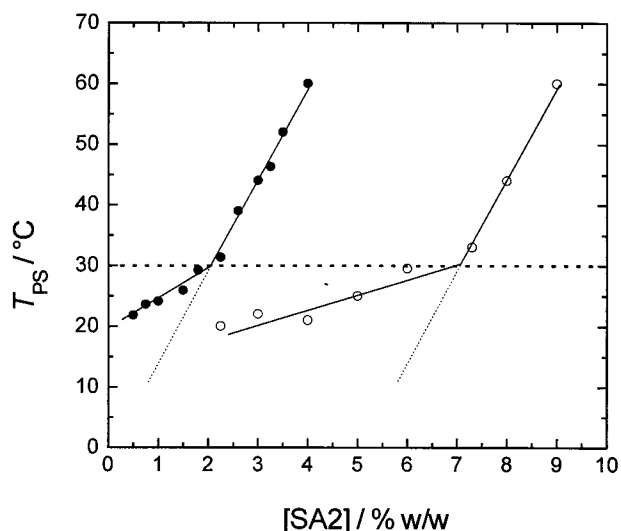


Figure 1. Phase separation temperatures estimated from turbidity measurements carried out during thermal ramping at 1 °C min⁻¹: filled circles, 4.5% w/w gelatin/maltodextrin in 0.1 M salt; open circles, 4% w/w gelatin/maltodextrin in deionized water.

a Reichert-Jung Ultracut E. The thin-sectioned samples were stained with uranyl acetate and lead citrate to visualize the gelatin phase and analyzed in a transmission electron microscope, LEO 906.

Rheology. Rheological measurements were performed using a Physica UDS 200 rheometer (Paar Physica, Stuttgart, Germany). A cup and bob geometry was used. A layer of mineral oil was applied on the surface of the sample in order to prevent evaporation. The frequency was 1 Hz and the strain 0.5% during the measurements. The sample was transferred to a preheated rheometer. The viscoelastic properties were recorded during the temperature quench and subsequently over relevant holding times at the final temperature. The quench rate used was approximately 20 °C min⁻¹ and was achieved by the switching of water baths supplying flow around a metal annulus in which the cup was housed.

Results and Discussion

Phase Separation. Phase separation in systems that have an upper critical solution temperature can be induced by a thermal step, either via a fast quench or via a controlled, continuous cooling procedure into the incompatibility region of the phase diagram. However, in practice, phase separation may not occur immediately upon crossing over the binodal into the metastable region, owing primarily to the finite kinetics of nucleation. The location of the binodal in the phase diagram is dependent on several factors including the ionic strength, pH, molecular weight, and interaction parameters of the individual polymers.⁴³

The main objective of this work is to study how the progressive conformational ordering of the gelatin influences the location of the binodal and hence the onset of phase separation. Conformational ordering is measured as the amount of helices by optical rotation. Estimates of the temperatures of phase separation of gelatin/maltodextrin systems, containing 4.5% and 4% w/w gelatin, in 0.1 M ionic strength solution and in deionized water, respectively, as a function of maltodextrin concentration, are shown in Figure 1. These have been obtained from turbidity measurements carried out during thermal ramping at 1 °C min⁻¹^{36,37} and confirmed by CLSM.² Both data sets change their slope at approximately 30 °C, which coincides with the tempera-

ture where gelatin starts to order.^{44,45} Between 60 and 30 °C, the dependence of the phase separation temperature on the maltodextrin concentration is approximately 15 °C/% w/w, whereas below about 30 °C, a much smaller concentration dependence is observed. These two domains can be classified as the "high-temperature" domain and the "low-temperature" domain, according to the initiation of phase separation.³⁵ It should be noted that the gradient of the plot below 30 °C is specific to 1 °C min⁻¹ and is dependent upon the scan rate. This section of the plot would continuously evolve toward the horizontal with decreasing rate of cooling.

The dotted lines in Figure 1 show extrapolations of the phase separation temperature estimates measured above 30 °C to temperatures below this. These lines show the estimated maltodextrin concentration (at fixed gelatin composition) through which the binodal passes at the corresponding temperature and, as such, serve as an estimate of the temperature dependence of the binodal, independent of the conformational ordering of gelatin. A comparison between the simple extrapolated temperature dependence below 30 °C with the actual data in Figure 1 shows that systems that normally would not phase separate according to the temperature dependence of the binodal will phase separate according to some additional driving force toward incompatibility.

Figure 1 also clearly shows that the miscibility of the biopolymers is altered as the ionic content of the mixture is changed. The compatibility of the charged gelatin and the neutral maltodextrin is increased as the salt concentration is decreased from 0.1 M salt to deionized water. This means that, at a constant gelatin concentration, in deionized water higher concentrations of maltodextrin are required in order to promote immiscibility than in 0.1 M salt. It has been argued that this change in compatibility is due to the entropic effect of dissociating counterions.⁴⁶ As the aim of this work is to study the effect of conformational ordering on phase behavior, experiments were performed in deionized water, since the region of concentration space in which mixtures are still initially miscible following quenches to temperatures below the ordering temperature of gelatin is increased compared to systems containing added salt.

The Additional Driving Force toward Incompatibility. Parts a and b of Figure 2 show the turbidity and optical rotation, measured simultaneously, for a 4% w/w gelatin/4% w/w maltodextrin system following a quench from 60 to 20 and to 25 °C, respectively. Parts c and d of Figure 2 show results from the same experiments carried out on a 4% w/w gelatin/3% w/w maltodextrin system. The measurement begins ($t = 0$) when the temperature of the system reaches 90% of the amplitude of the change to the quench temperature. It is clear that significant turbidity increases, as a result of phase separation, are only observed after significant delay periods. Results obtained from turbidity measurements in solutions containing added salt show the same effect.³⁷ Figure 2a–d also demonstrates that the amount of gelatin helices is increasing during this time, prior to the observation of the turbidity increase. It is important to note that changes in optical rotation due to the effects of thermal quenching on the optical activity of maltodextrin and the cell windows were measured in control experiments (solutions without gelatin) and have already been subtracted from the data shown in Figure 2. In addition, Figure 2a–d also shows that the rate of helix formation is temperature-depend-

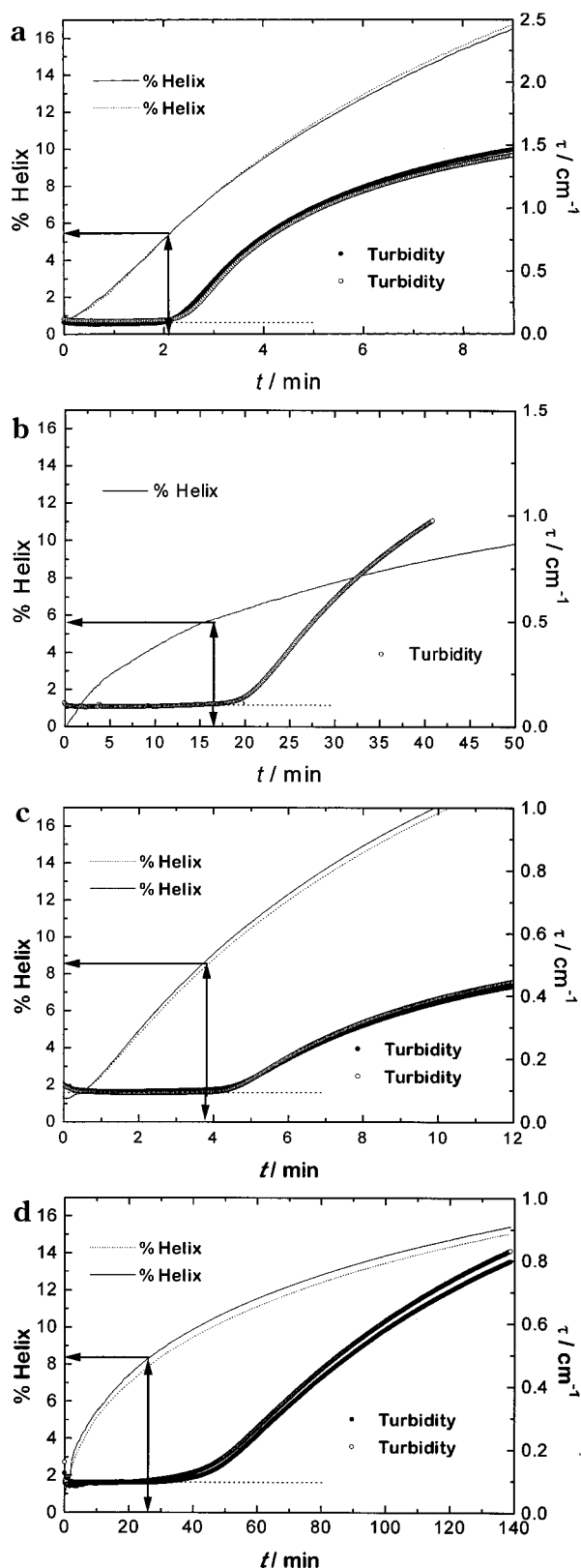


Figure 2. (a) Turbidity and optical rotation measured simultaneously for a 4% w/w gelatin/4% w/w maltodextrin mixture following a quench to 20 °C. Two data sets are shown. (b) Turbidity and optical rotation measured simultaneously for a 4% w/w gelatin/4% w/w maltodextrin mixture following a quench to 25 °C. (c) Turbidity and optical rotation measured simultaneously for a 4% w/w gelatin/3% w/w maltodextrin mixture following a quench to 20 °C. Two data sets are shown. (d) Turbidity and optical rotation measured simultaneously for a 4% w/w gelatin/3% w/w maltodextrin mixture following a quench to 25 °C. Two data sets are shown.

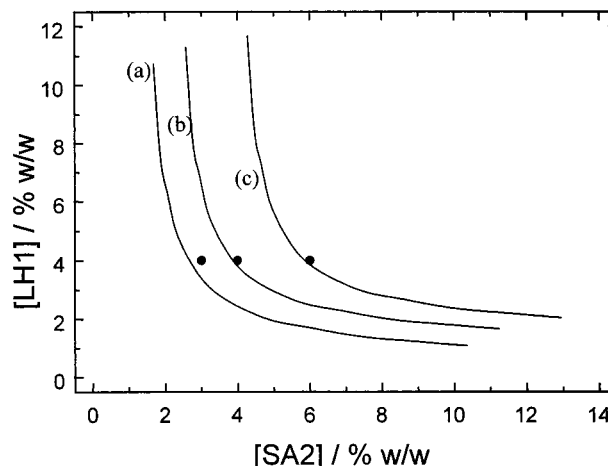


Figure 3. Schematic phase diagram of the gelatin/maltodextrin system at 25 °C. Binodals are shown as a function of percent gelatin helix formation. (a) 8.5%, (b) 5.5%, and (c) 0%. Solid circles are compositions studied in turbidity/OR experiments.

ent and increases with decreasing temperature, in agreement with earlier studies of helix formation of gelatin.⁴⁵ The percentage of gelatin helices, obtained from the optical rotation measurements, was calculated at the time of the initiation of phase separation. This time was obtained from the point at which the value of the turbidity was judged to have left its baseline. In each case, the baseline was obtained by averaging the initial level of turbidity and departure from it was determined by a value being different from the baseline by $>0.005 \text{ cm}^{-1}$. This value was judged to provide a reasonable criterion based on magnitude of the experimental noise.

Figure 2a shows that at 20 °C approximately 5.5% helix formation is present at the time when the 4% w/w gelatin/4% w/w maltodextrin system begins to phase separate, as indicated by the increase in turbidity after about 2 min. It can also be seen in Figure 2b that, at 25 °C, the delay time for the same system is about 17 min. However, at both 20 and 25 °C the system exhibits approximately 5.5% helix formation at the time it begins to phase separate. This is strong evidence of a causal link between the development of a particular amount of conformational order and the onset of phase separation. The hypothesis is strengthened by examining the results shown in Figure 2c,d obtained from the 4% w/w gelatin/3% w/w maltodextrin system at the same two temperatures. While phase separation is initiated after approximately 4 min at 20 °C and 26 min at 25 °C, the percentage of gelatin helices at the onset of phase separation is once again approximately the same (8.5% in this case). The composition of 4% w/w gelatin/3% w/w maltodextrin is intrinsically more compatible than 4% w/w gelatin/4% w/w maltodextrin, and as such, longer delay times are observed at both temperatures, corresponding to a larger amount of helix formation being necessary before phase separation is invoked.

Figure 3 shows a schematic phase diagram at 25 °C with and without gelatin ordering. While the shape of the curve is schematic, the points in the diagram indicate the compositions of the systems studied by turbidity/OR and changes in position of the hypothetical binodal with the percentage of gelatin helices are shown in order to be consistent with the data reported. The binodals will shift somewhat toward increased incompatibility with reducing temperature. The small mag-

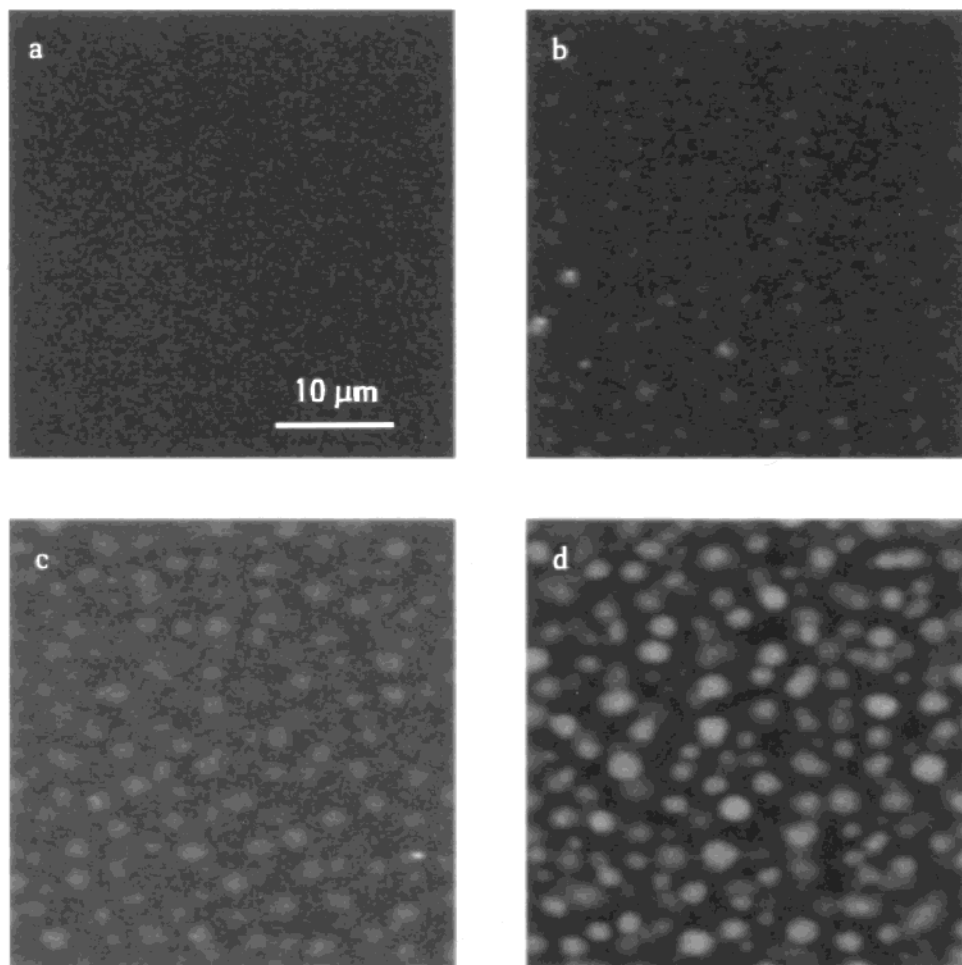


Figure 4. A time sequence of CLSM micrographs at 4% w/w gelatin/4% w/w maltodextrin quenched to 20 °C. The micrographs are shown after (a) 1, (b) 3, (c) 4, and (d) 29 min.

nitude of such a shift, as illustrated by the extrapolated temperature dependence in Figure 1, clearly explains the measured similarity between the percentage of gelatin helices required for the onset of phase separation at 20 and 25 °C.

The Time Dependence of the Onset of Phase Separation. To visualize the evolution of the system morphology, a sequence of CLSM micrographs were obtained from a 4% w/w gelatin/4% w/w maltodextrin system without added salt following a quench to 20 °C. The micrographs are shown in Figure 4 and serve to illustrate how the microstructure develops with time, from a miscible system to a phase-separated state that is kinetically trapped by gelation. Micrograph 4a shows the system after 1 min at 20 °C, which has not phase separated. However, after a delay time of 3 min at 20 °C several diffuse maltodextrin inclusions have appeared as shown in micrograph 4b. This means that the phase separation has been initiated. In addition, the delay time prior to the onset of demixing observed by CLSM is in close agreement with the delay time of 2 min obtained by turbidimetry shown in Figure 2a. It can be seen in micrograph 4c that the maltodextrin inclusions have grown and become more distinct after 4 min at 20 °C when compared to micrograph 4b. Finally, micrograph 4d displays the microstructure after 29 min at 20 °C, when the phase-separated inclusions have been kinetically trapped by the gelation of the continuous gelatin-rich phase. After this time no sub-

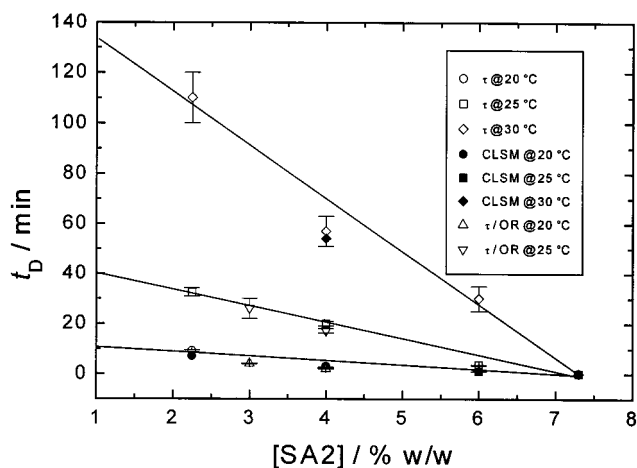


Figure 5. Time delays (t_D) observed prior to phase separation, measured by turbidity, turbidity/OR, and confocal laser scanning microscopy, in 4% w/w gelatin/maltodextrin mixtures at various quench temperatures.

sequent changes in the morphology could be detected by CLSM.

To achieve some increased understanding of the rate of binodal movement generated by the gelatin ordering process, further experiments were carried out on a number of systems of different maltodextrin concentration, quenched to different temperatures. Time delays observed prior to the onset of phase separation, determined by turbidity, turbidity/OR, and CLSM, are shown

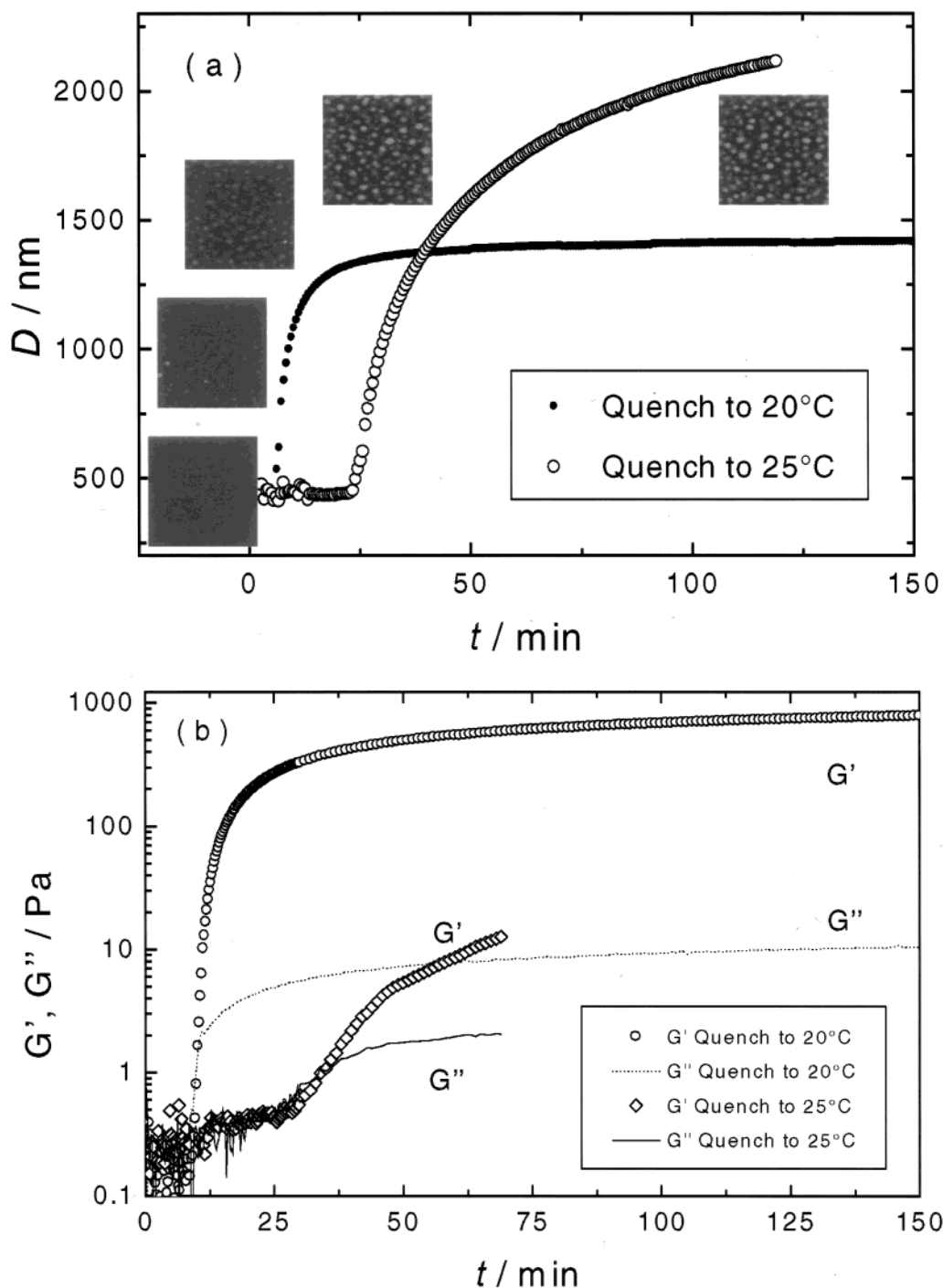


Figure 6. Time evolution of (a) the estimated evolution of particle sizes, obtained from turbidity measurements, shown with corresponding CLSM micrographs at 1, 3, 4, 25, and 29 min and (b) the storage modulus (G') and loss modulus (G'') for 4% w/w gelatin/4% w/w maltodextrin following temperature quenches to 20 and 25 °C.

in Figure 5 as a function of maltodextrin concentration at various quench temperatures. The error bars are estimates obtained from the ranges observed in repeated turbidity experiments. Values of the delay times from all the techniques show good agreement and the delay time is seen to increase with increasing quench temperature. A linear regression analysis of the delay time versus maltodextrin concentration data at 20, 25, and 30 °C was performed, and the results are plotted in Figure 5. The delay time decreases with increasing maltodextrin concentration, and it is interesting to note that the regressions at each temperature give an intercept (zero delay time) at close to 7.3% w/w maltodextrin concentration, where indeed the system is

intrinsically immiscible above the ordering temperature of gelatin, as can be seen from Figure 1. Although there is no strict theoretical basis for such a linear functional form, the slope of these regression lines gives first estimates of 0.48, 0.15, and 0.05% w/w min⁻¹ for the rate of binodal movement at 20, 25, and 30 °C, respectively. This shows that the rate of binodal movement increases with decreasing temperature, consistent with expectations of the change of percent helix with time from the kinetics of gelatin ordering.^{40,44,45}

Binodal Evolution and the Mechanism of Phase Separation Induced by Conformational Ordering of Gelatin. The preceding sections have provided evidence that the onset of phase separation is dependent

on the conformational ordering of gelatin. Accordingly, it is interesting to consider the process by which ordering influences the thermodynamics of the mixed system. In general, the miscibility of mixed biopolymer systems of varying composition is determined by their position relative to the system binodal, which can be modeled within the framework of the Flory–Huggins lattice model. This approach has been used to model the phase behavior of polymer mixtures and ternary, biopolymer/solvent systems.⁴⁶ The model is essentially cast in terms of the relative molar volumes of the biopolymers and a set of so-called χ parameters that are related to the second virial coefficients and embody the interaction of the biopolymers with the solvent and with each other. Any perturbation of any of these parameters can potentially modify the system thermodynamics. Within this framework the concept of conformational changes inducing phase separation has previously been suggested.^{2,28} However, a detailed calculation of the time course of the binodal, generated by gelatin ordering, is elusive, as the way in which the molecular weight and interaction parameters will change as the percentage of helix formation increases is unknown. However, by changing the molecular weight (number-average molar mass) in the Flory–Huggins lattice model, it is possible to demonstrate that it is unlikely that a molecular weight increase of gelatin alone is the primary driving force behind ordering-induced phase separation. Although polydispersity will complicate such a calculation, it is unlikely that its inclusion would alter this conclusion. In addition, it is known that the $\chi_{\text{LH-H}_2\text{O}}$ value changes upon ordering in a direction that would increase system compatibility; i.e., it becomes more like $\chi_{\text{SA}_2\text{-H}_2\text{O}}$.³⁷ It is possible then to attribute the increased incompatibility to a combination of molecular weight increase and changes in $\chi_{\text{LH-SA}_2}$, which characterizes the interaction between the two biopolymers.

Phase Separation during Ordering and Network Formation. In an attempt to examine how the rheological changes will impact on the microstructural development, an estimate of the size evolution of included phases, obtained from fitting turbidity spectra,³⁶ has been compared with the evolution of viscoelastic properties measured using small deformation mechanical spectroscopy. Figure 6a shows the estimated evolution of the sizes of the maltodextrin inclusions, obtained from turbidity measurements carried out as a function of wavelength, for the 4% w/w gelatin/4% w/w maltodextrin system following temperature quenches to 20 and 25 °C. In addition, CLSM micrographs are included in order to visualize the evolution of the microstructure. The micrographs are those shown in Figure 4 with the addition of a further micrograph of the kinetically trapped system taken at a different location in the sample. The micrographs display the microstructure after 1, 3, 4, 25, and 29 min at 20 °C. The fitting of the turbidity spectra data³⁶ was good ($r^2 > 0.995$), and extracted size values were found to be in reasonable agreement with those obtained from the CLSM micrographs (1.4 vs 2 μm after 29 min, respectively).

Figure 6b shows the evolution of the dynamic storage and loss moduli under the same conditions as in Figure 6a. The crossover of the storage modulus G' and the loss modulus G'' , i.e., when the phase angle $\delta = 45^\circ$, at 1 Hz was used to register the gel transition. This definition is commonly used in the biopolymer literature, and

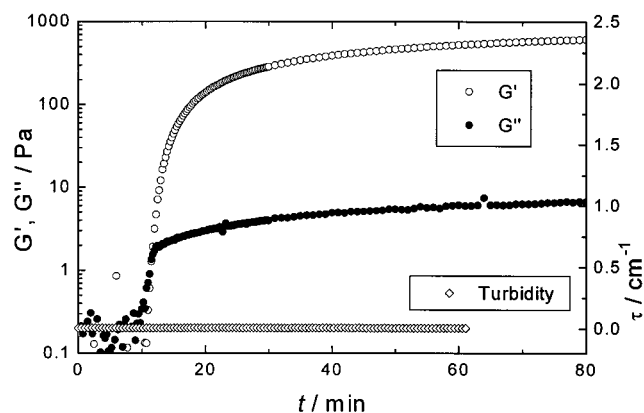


Figure 7. Turbidity and the storage modulus (G') and the loss modulus (G'') as a function of time for a 4% w/w gelatin/1.5% w/w maltodextrin mixture following a temperature quench to 20 °C.

discrepancies between this point and that obtained using the more precise determination of the gel point, as measured over a wide frequency range,^{47–49} are not significant enough to affect the conclusions drawn below. By comparing parts a and b of Figure 6, it can be seen that the size of the maltodextrin inclusions continues to evolve even after the gel transition (G' , G'' crossover times from Figure 6b are 10 and 35 min at 20 and 25 °C, respectively), in agreement with earlier studies.^{45,50} The growth of the inclusions, as determined by turbidity measurements, does, however, stop after about 30 min at 20 °C. In addition, the last two CLSM micrographs in Figure 6a show little microstructure coarsening after 25 min at this temperature. Figure 6b shows that this corresponds to a gel strength of the order of a couple of 100 Pa. It can clearly be seen that the evolution of the size of the maltodextrin inclusions at 25 °C continues for a considerably longer time than at 20 °C. Although the gel point is passed, the reduced rate of gelation at the higher temperature means that for a considerable time the elasticity of the system is lower than that found at 20 °C, and the inclusions can continue to grow.

The OR and turbidity data suggest that as the maltodextrin concentration is decreased, an increased amount of helices is required to form in order to induce incompatibility. However, for the mixtures discussed thus far, phase separation has always been observed. This shows that the critical helix content required to induce phase separation has been below the amount necessary for gelatin sols to build up a sufficient viscosity, or to percolate into a gelatin network of sufficient elasticity, to prevent phase separation. Consequently, by decreasing the maltodextrin concentration, a concentration may be reached where the network elasticity is sufficient to prevent phase separation before the amount of helices reaches the level required for initiation of demixing.

In an attempt to test this hypothesis, the effect of conformational ordering of gelatin and the network elasticity was investigated at low maltodextrin concentration. Mixtures of 4% w/w gelatin and 1.5% w/w maltodextrin were quenched from 60 to 20 °C and subjected to viscoelastic and turbidity measurements. Figure 7 shows the turbidity, storage modulus G' , and the loss modulus G'' as a function of time. The crossover of the storage modulus G' and the loss modulus G'' appears after about 12 min, which means that the

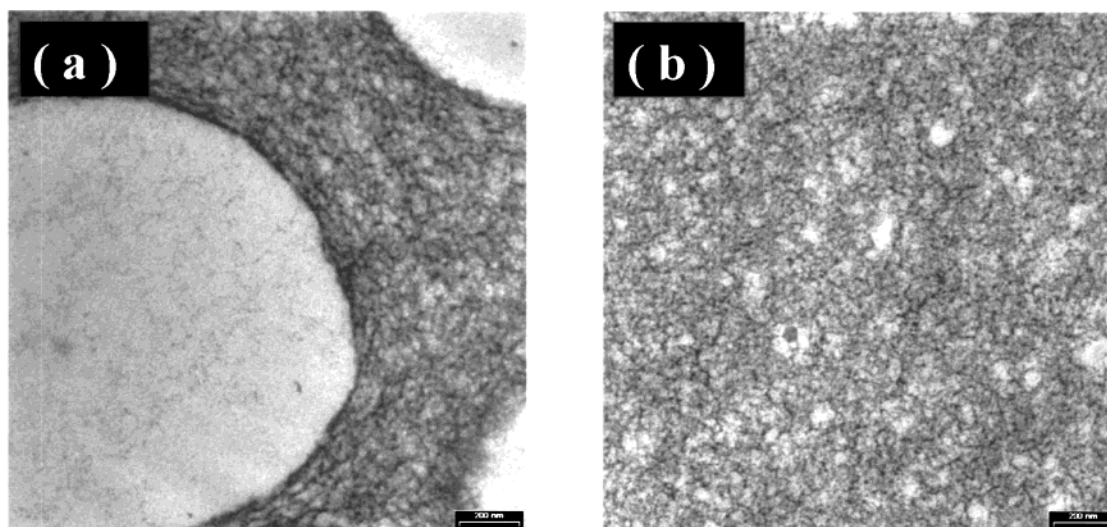


Figure 8. Transmission electron micrographs of systems (a) 4% w/w gelatin/4% w/w maltodextrin and (b) 4% w/w gelatin/1.5% w/w maltodextrin following a temperature quench to 20 °C. The scale bar is 200 nm.

gelatin network has started to percolate the whole system. The turbidity measurement in Figure 7 clearly shows that no phase separation has occurred after 60 min. This means either that the system is still compatible because the amount of ordering formed is less than that required to induce phase separation or that the energy required for the deformation of the gelatin network formed has prevented phase separation.

It is interesting to consider the morphology of such a system at a smaller distance scale, and accordingly transmission electron microscopy experiments have been carried out. Figure 8 shows TEM micrographs obtained 3 h after quenches to 20 °C. The dark areas are the gelatin network. Micrograph 8a shows the microstructure for a 4% w/w gelatin/4% w/w maltodextrin mixture, which has been observed to phase separate by turbidity and CLSM. It shows large maltodextrin inclusions inside a continuous gelatin-rich phase. Micrograph 8b shows the microstructure of a 4% w/w gelatin/1.5% w/w maltodextrin system, which is not observed to phase separate by turbidity and CLSM. It can be seen that the microstructure of this system is comparable to that of the gelatin-rich continuous phase in the incompatible system. Both micrographs reveal that there exist density fluctuations inside the continuous gelatin-rich phase. This can be seen as light, irregular domains in the gelatin network. Maltodextrin is known to form evenly sized, semicrystalline starch aggregates.⁵¹ Some of these aggregates can be seen as isolated dense particles inside the gelatin network in micrograph 8b.

Conclusions

Simultaneous turbidity and optical rotation measurements have demonstrated that the conformational ordering of gelatin can induce phase separation in gelatin/maltodextrin mixtures. The fact that the same amount of gelatin helices are found at the onset of phase separation at 20 and 25 °C, but after significantly different delay times, provides strong evidence that it is the formation of a particular degree of gelatin ordering that is responsible for the initiation of phase separation.

It was found from rheology, turbidity, and CLSM measurements that the classically defined gel point

($G' = G''$) should not be taken in isolation as evidence of the immediate freezing of the system microstructure. It was also found that, for sufficiently low maltodextrin concentrations, no phase separation was obtained. In this case either the system is still compatible because the amount of ordering formed is less than that required to induce phase separation or the elasticity of the network formed (many hundred Pa) has prevented demixing. In addition, TEM showed that the microstructure of such a system is comparable with that of the gelatin-rich phase of an incompatible system.

In future work, image analysis techniques will be used in conjunction with CLSM to perform a more detailed characterization of the morphology as a function of time. Ordering-induced phase separation will be explored further in other mixtures, where the conformational transition of another polymer, with different ordering kinetics, is used to trigger the separation process.

Acknowledgment. This study has been carried out with the financial support from the Commission of the European Communities, Agriculture and Fisheries (FAIR), specific RTD program, CT 96 1015, "Mixed Biopolymers—Mechanism and Application of Phase Separation". It does not necessarily reflect its views and in no way anticipates the Commission's future policy in the area. Special thanks are extended to A. Altskär for help with the preparation of the covalently stained maltodextrin and transmission electron microscopy and to D. Fabri for helping to carry out the turbidity experiments. Financial support from TFR, the Swedish Research Council for Engineering Science, is gratefully acknowledged by Niklas Lorén.

References and Notes

- (1) Tromp, R. H.; Rennie, A. R.; Jones, R. A. L. *Macromolecules* **1995**, *28*, 4129–4138.
- (2) Lorén, N.; Hermansson, A.-M. *Int. J. Biol. Macromol.* **2000**, *27*, 249–262.
- (3) Alevisopoulos, S.; Kasapis, S.; Abeysekera, R. *Carbohydr. Res.* **1996**, *293*, 79–99.
- (4) Sciortino, F.; Bansil, R.; Stanley, H. E.; Alstrom, P. *Phys. Rev. E* **1993**, *47* (6), 4615–4618.
- (5) Schulz, M.; Paul, B. *Phys. Rev. B* **1998**, *58* (17), 11096–11098.
- (6) Asnaghi, D.; Giglio, M.; Bossi, A.; Righetti, P. G. *J. Mol. Struct.* **1996**, *383*, 37–42.

- (7) Graham, P. D.; Pervan, A. J.; Mchugh, A. J. *Macromolecules* **1997**, *30*, 1651–1655.
- (8) Bansil, R.; Lal, J.; Carvalho, B. L. *Polymer* **1992**, *33* (14), 2961–2969.
- (9) Bansil, R.; Liao, G. *Trends Polym. Sci.* **1997**, *5* (5), 146–154.
- (10) Tanaka, F. *Prog. Colloid Polym. Sci.* **1997**, *106*, 158–166.
- (11) Khomutov, L. I.; Lashek, N. A.; Ptitchkina, N. M.; Morris, E. R. *Carbohydr. Res.* **1995**, *28*, 341–345.
- (12) Clark, A. H. In *Biopolymer Mixtures*; Harding, S. E., Hill, S. E., Mitchell, J. R., Eds.; Nottingham University Press: Nottingham, 1995; pp 37–64.
- (13) Tromp, R. H.; Jones, R. A. L. *Macromolecules* **1996**, *29*, 8109–8116.
- (14) Lundin, L.; Odic, K.; Foster, T. J.; Norton, I. T. In *Proceedings of Supramolecular and Colloidal Structures in Biomaterials and Biosubstrates*; Mysore: India, RSC, in press.
- (15) Lorén, N.; Langton, M.; Hermansson, A.-M. *Food Hydrocolloids* **1999**, *13*, 185–198.
- (16) Kasapis, S.; Morris, E. R.; Norton, I. T.; Gidley, M. J. *Carbohydr. Polym.* **1993**, *21*, 249–259.
- (17) Barton, B. F.; Graham, P. D.; McHugh, A. J. *Macromolecules* **1998**, *31*, 1672–1679.
- (18) Cavanaugh, T. J.; Nauman, E. B. *J Polym. Sci., Polym. Phys.* **1998**, *36*, 2191–2196.
- (19) Delville, J. P.; Lalaude, C.; Buil, S.; Ducasse, A. *Phys. Rev. E* **1999**, *59*, 5804–5818.
- (20) Kojima, J.; Takenaka, M.; Nakayama, Y.; Hashimoto, T. *Macromolecules* **1999**, *32*, 1809–1815.
- (21) Barton, B. F.; McHugh, A. J. *J. Polym. Sci., Polym. Phys.* **1999**, *37*, 1449–1460.
- (22) Graham, P. D.; Barton, B. F.; McHugh, A. J. *J. Polym. Sci., Polym. Phys.* **1999**, *37*, 1461–1467.
- (23) Tran-Cong, Q.; Kawai, J.; Endoh, K. *Chaos* **1999**, *9*, 298–307.
- (24) Ohta, T.; Urakawa, O.; Tran-Cong, Q. *Macromolecules* **1998**, *31*, 6845–6854.
- (25) Chou, Y. C.; Lee, L. J. *Polym. Eng. Sci.* **1994**, *34*, 1239–1249.
- (26) Harada, A.; Tran-Cong, Q. *Macromolecules* **1996**, *29*, 4801–4803.
- (27) Harada, A.; Tran-Cong, Q. *Macromolecules* **1997**, *30*, 1643–1650.
- (28) Elicabe, G. E.; Larrondo, H. A.; Williams, R. J. J. *Macromolecules* **1998**, *31*, 8173–8182.
- (29) Elicabe, G. E.; Larrondo, H. A.; Williams, R. J. J. *Macromolecules* **1997**, *30*, 6550–6555.
- (30) Okada, M.; Sakaguchi, T. *Macromolecules* **1999**, *32*, 4154–4156.
- (31) Kyu, T.; Mustafa, M.; Yang, J.-C.; Kim, J. Y.; Palfy-Muhoray, P. In *Polymer Solutions, Blends, and Interfaces*; Noda, I., Rubingh, D. N., Eds.; Elsevier Science: Amsterdam, 1992; p 245.
- (32) Chan, P. K.; Rey, A. D. *Macromolecules* **1996**, *29*, 8934–8941.
- (33) Chan, P. K.; Rey, A. D. *Macromolecules* **1997**, *30*, 2135–2143.
- (34) Zhang, J.; Zhang, H.; Yang, Y. *J. Appl. Polym. Sci.* **1999**, *72*, 59–67.
- (35) Lundin, L.; Norton, I. T.; Foster, T. J.; Williams, M. A. K.; Hermansson, A.-M.; Bergström, E. In *Gums and Stabilisers for the Food Industry 10*; Williams, P. A., Phillips, G. O., Eds.; The Royal Society of Chemistry: Cambridge, 2000; pp 167–180.
- (36) Aymard, P.; Williams, M. A. K.; Clark, A. H.; Norton, I. T. *Langmuir* **2000**, *16* (19), 7383–7391.
- (37) Williams, M. A. K.; Fabri, D.; Hubbard, C. D.; Lundin, L.; Foster, T. J.; Clark, A. H.; Norton, I. T.; Lorén, N.; Hermansson, A.-M.; Leisner, D.; Lopez-Quintela, M. A. Submitted to *Langmuir*.
- (38) Lloyd, D. K.; Goodall, D. M.; Scrivener, H. *Anal. Chem.* **1989**, *61*, 1238–1243.
- (39) Lloyd, D. K.; Goodall, D. M. *Chirality* **1989**, *1*, 251–264.
- (40) Djabourov, M.; Leblond, J.; Papon, P. *J. Phys. (Paris)* **1988**, *49*, 319–332.
- (41) Garnier, C.; Bourriot, S.; Doublier, J.-L. In *Gums and Stabilisers for the Food Industry*; Williams, P. A., Phillips, G. O., Eds.; The Royal Society of Chemistry: Cambridge, 1998; Vol. 9, pp 247–256.
- (42) De Belder, A. N.; Granath, K. *Carbohydr. Res.* **1973**, *30*, 375.
- (43) Zasyupkin, D. V.; Braudo, E. E.; Tolstoguzov, V. B. *Food Hydrocolloids* **1997**, *11*, 159–179.
- (44) Djabourov, M. *Contemp. Phys.* **1988**, *29* (3), 273–297.
- (45) Djabourov, M.; Maquet, J.; Theveneau, H.; Papon, P. *Br. Polym. J.* **1985**, *17*, 169–174.
- (46) Piculell, L.; Bergfeldt, K.; Nilsson, S. In *Biopolymer Mixtures*; Harding, S. E., Hill, S. E., Mitchell, J. R., Eds.; Nottingham University Press: Nottingham, 1995; pp 13–35.
- (47) Chambon, F.; Winter, H. H. *Polym. Bull.* **1985**, *13*, 499–503.
- (48) Winter, H. H.; Chambon, F. *J. Rheol.* **1985**, *30*, 367–382.
- (49) Winter, H. H.; Chambon, F. *Polym. Eng. Sci.* **1987**, *27*, 1698–1702.
- (50) Te Nijenhuis, K. *Colloid Polym. Sci.* **1981**, *259*, 1017–1026.
- (51) Clark, A. H.; Eyre, S. C. E.; Ferdinando, D. P.; Lagarrigue, S. *Macromolecules* **1999**, *32*, 7897–7906.

MA0013051